ABSTRACT: Prolonged exposure to hand-transmitted vibration can cause debilitating neural and vascular dysfunction in humans. It is unclear whether the pathophysiology involves simultaneous or sequential injury of arteries and nerves. The mechanism of vibration injury was investigated in a rat tail model, containing arteries and nerves structurally similar to those in the human hand. Tails were selectively vibrated for 1 or 9 days with the remainder of the animal at rest. One vibration bout of 4 h/day, 60 Hz, 5 g (49 m/s^2) acceleration, injured endothelial cells. Injury was signaled by elevated immunostaining for NFATc3 transcription factor. Electron microscopy revealed that vibration for 9 days produced loss and thinning of endothelial cells, with activated platelets coating the exposed subendothelial tissue. Endothelial cells and arterial smooth muscle cells contained double membrane–limited, swollen processes indicative of vasoconstriction-induced damage. Laser doppler surface recording demonstrated that 5 min of vibration significantly diminished tissue blood perfusion. These findings indicate that early injury involves vasoconstriction and denuding of the arterial endothelium.
 Muscle Nerve **25:** 527–534, 2002

VIBRATION INJURY DAMAGES ARTERIAL ENDOTHELIAL CELLS

BRIAN D. CURRY, MS,[1] JAMES L.W. BAIN, BA,[1] JI-GENG YAN, MD,[2] LIN LING ZHANG, MD,[2] MARK YAMAGUCHI, BS,[2] HANI S. MATLOUB, MD,[2] and DANNY A. RILEY, PhD[1]

[1]Department of Cell Biology, Neurobiology, and Anatomy, Medical College of Wisconsin, 8701 Watertown Plank Road, Milwaukee, Wisconsin 53226, USA
[2]Department of Plastic Surgery, Medical College of Wisconsin, Milwaukee, Wisconsin, USA

Accepted 5 November 2001

In America, 8–10 million workers are exposed daily to vibration from powered tools.[32] Prolonged exposure to excessive, hand-transmitted vibration may cause debilitating vascular, neurological, and musculoskeletal problems.[1,3,5,6,16,20,21,27,28] Many symptoms persist for years after cessation of tool use.[17] In 1918, Alice Hamilton investigated hand-arm symptoms of Indiana quarry stone-cutters and defined their vibration-induced condition as a secondary Raynaud's phenomenon of occupational origin.[8] The condition is now called the hand-arm vibration syndrome (HAVS). Although the late-stage pathophysiology of HAVS is well characterized, the onset and progression of the disease to an irreversible condition is poorly understood at the cellular and molecular levels. It is unknown whether the neurological symptoms that include tingling, numbness, and loss of dexterity are primary or secondary to the vascular symptoms of vasospasm and ischemia.[12] Also unknown are the initial cell types injured by vibration in either tissue. The purpose of the present study was to determine the early effects of vibration on arteries.

The understanding of early vibration injury has languished partly from the lack of satisfactory animal models for elucidating basic mechanisms and evaluating the efficacy of countermeasures. A number of models of vibration injury, including our initial attempts, vibrated either the hind limbs or the animal's entire body for days and caused significant structural and functional damage.[14,31] Although unequivocally achieving vibration injury of arteries and nerves, the complex anatomical organization of the nerves, blood vessels, muscles, and bones in the limbs complicated identification of the primary mechanisms. Okada addressed this concern by selec-

Abbreviations: B&K, Brüel and Kjaer; EC, endothelial cell; EM, electron microscopy; HAVS, hand-arm vibration syndrome; internal elastic membrane; LM, light microscopy; NFAT, nuclear factor of activated T cell; SMC, smooth muscle cell
Key words: hand-arm vibration syndrome; NFAT transcription factor; occupational disease; Raynaud's phenomenon; vasospasm
Correspondence to: D.A. Riley; e-mail: dariley@mcw.edu

Published online 19 February 2002 in Wiley InterScience (www.interscience.wiley.com). DOI 10.1002/mus.10058

tively vibrating the rat's tail with the remainder of the animal at rest.[18] This approach significantly reduced confounding variables that would potentially interfere with resolving early cellular alterations. The model is of additional value because of the structural similarities of arteries and nerves in the rat tail and human hand. Both appendages are moved by extrinsic muscles with long tendons and contain intrinsic skeletal muscles, mixed peripheral nerves, and a rich vascular network (Fig. 1A).[29,34]

Unlike Okada's study which focused on end-stage HAVS, the present study utilized the rat tail vibration model for investigating early arterial cell injury, resolved by electron microscopy (EM) and immunostaining for the Ca^{+2} activated transcription factor, nuclear factor of activated T cell (NFAT), an indicator of cell injury. The present study shows that endothelial cell disruption is an early event of vibration injury, and laser doppler tissue blood flow monitoring implicates vibration-induced vasoconstriction in the pathophysiology.

MATERIALS AND METHODS

Animal Groups. Forty male Sprague-Dawley rats (287 ± 20 g) were randomly assigned to five groups with eight rats per group: normal nontreated controls, 1-day sham controls, 1-day vibrated test animals, 9-day sham controls, and 9-day vibrated test animals. The rats were housed in vivarium plastic box cages in an animal holding room at 25°C and a 12/12 h, dark/light cycle. During vibration treatment, rats were placed individually in restraint tubes on a nonvibrating platform, and their tails were held with slight compression against a vibrating stage (Fig. 1A,B). Sham control rats were processed concurrently with vibrated animals. The sham controls were handled analogously except that their tails were held against a nonvibrating platform. Animal treatment, surgical interventions, and husbandry procedures were approved by the Medical College of Wisconsin's Animal Care Committee and complied with the Laboratory Animal Welfare Act.

Vibration. The sham and vibrated rats adapted to the restraining tubes on the first day, with most animals sleeping during the 4-h sessions conducted from 8AM–noon during the light period. The restraining tube was manufactured in-house from 2-inch internal diameter PVC pipe. The tube enclosed the body and a wire-mesh cage surrounded the head (Fig. 1B). Drilled holes permitted air exchange and gravity-fed exiting of urine and feces. The restraining chamber was bolted to a nonvibrating platform which was separated from the vibration platform by a 1 cm gap. Custom form-fitted, plastic splint molds (Polyform, Smith & Nephew, London, UK) confined the tails by slight compression to the linear vibration platform in a one-to-one frequency correspondence. To form-fit a splint to the tail, the plastic was softened in 100°C water. While pliable but not too warm to cause discomfort, the plastic was sculpted around the tail until it rehardened as it cooled. During vibration, the splints were affixed to the vibration platform with Velcro strips.

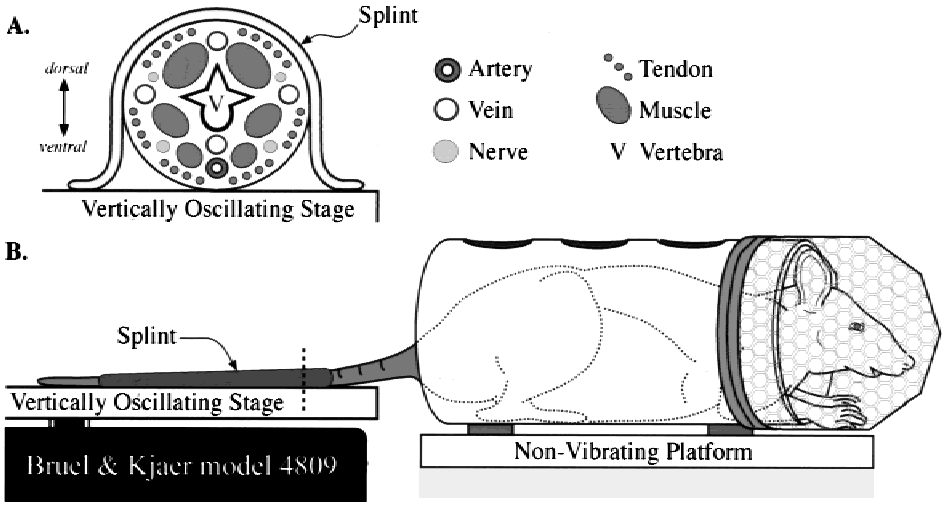

FIGURE 1. (A) A cross-section of a typical caudal segment of the rat's tail at the level of the dashed line in panel (B) contains a central vertebra, six intrinsic skeletal muscles, four large nerve trunks, four major veins, a ventral artery, and bundles of tendons from extrinsic muscles. The artery is recessed from the surface and not subjected to direct mechanical impact trauma from the vibration platform. **(B)** During vibration, the nonanesthetized rat is confined within a tubular cage anchored to a nonvibrating platform. The animal's tail bridges a gap and is affixed to the vibrating stage by a form-fit plastic splint.

Vibration consisted of linear vertical oscillations of 60 Hz and 5 g acceleration (49 m/s^2) for 4 h/day for either 1 or 9 days. During a standard 4-h bout, acceleration drifted < 2 m/s^2, and frequency shifted < 1 Hz. Acceleration of the nonvibrating platform was < 1 m/s^2. Accelerometer placement on the tail measured 5 g acceleration, indicating tight coupling to the accelerating platform. The electromagnetic vibration accelerator, a Brüel and Kjaer (B&K) PM Vibration Exciter type 4809 (Naerum, Denmark), was driven by a Simpson 420 Function Generator (Elgin, Illinois) in sine wave form. The signal was augmented by a B&K Power Amplifier type 2706. Frequency and acceleration were checked daily with an HP 1201B oscilloscope and a B&K accelerometer mounted on a B&K Integrating Vibration Meter, type 2513.

Tail Tissue Blood Perfusion. Five additional male rats (266 ± 6 g) were used for measurements of tissue blood perfusion of the tails for 10 min before and 10 min immediately after 5 min of vibration, using a Transonic System Inc. (Ithaca, New York) BLF 21 laser doppler apparatus coupled to a Gould (Cleveland, Ohio) Brush 220 chart recorder. The doppler probe was recessed in the vibration platform to provide a level surface for the tail and positioned against the ventral surface of caudal tail segment C7. The effect of vibration on tissue perfusion was tested statistically by comparing the before- and after-vibration values using a paired *t*- test for repeated measures with $P < 0.05$ considered significant. Data are presented as mean ± SEM.

Tissue Processing. Rats were deeply anesthetized with a ketamine 72 mg/kg, xylazine 12 mg/kg, and acepromazine 0.09 mg/kg mixture injected into the quadriceps muscle. The tail skin was removed, and caudal segments C5–C8 were excised distally to proximally by cutting through the intervertebral joints with a scalpel. The isolated segments were placed in either 4% paraformaldehyde fixative in a 0.1 M phosphate buffer (pH 7.4) at 20°C for 2 h for light microscopy (LM) or 4% glutaraldehyde, 2% paraformaldehyde, cacodylate (pH 7.4) fixative for electron microscopy (EM). The ventral tail artery was immersion fixed in situ to minimize dissection artifacts. For LM, fixed segments were rinsed three times and stored refrigerated in 0.1 M phosphate buffer (pH 7.4). The following day, ventral arteries were microdissected from each segment and cryoprotected in a graded series of sucrose buffers: 10% for 20 min and 20% for 45 min at 20°C, and 30% at 5°C for 24 h. Cryoprotected arteries were embedded in Sakura's Tissue-Tek O.T.C. (Torrance, CA), quick frozen in a Freon 22 (LaRoche Chemicals, Baton Rouge, LA) slurry cooled by liquid N_2 and stored in liquid N_2. EM-fixed arteries were cut into smaller pieces, postfixed for 1 h in 1.3% osmium tetraoxide, and embedded in epoxy resin for semithin and ultrathin sectioning.

Immunohistochemistry. The frozen fixed arteries were cryostat-sectioned at 6 μm and immunostained with primary antibodies directed against Nuclear Factor of Activated T cell c3 (NFATc3) (1:300; Santa Cruz Biotechnology, Santa Cruz, California). Omission of the primary antibody was performed to control for nonspecific labeling of secondary antibodies. Nonspecific binding was reduced by blocking with 1.5% normal goat serum. FITC biotin conjugated, secondary antibodies were obtained from Vector Laboratories (Burlingame, California). Caudal segments C5 through C8 were compared within each animal to insure no segmental differences existed. Immunofluorescence photomicrographs were taken with a Nikon (Tokyo, Japan) Optiphot-2 epifluorescence microscope fitted with appropriate excitation and barrier filters and a Diagnostic Instruments SPOT CCD camera (Sterling Heights, Michigan). Contrast and brightness of images were optimized with Metamorph (West Chester, Pennsylvania) imaging software.

Positive Immunostaining Control for a Marker of Mechanical Cell Injury. The ability of mechanical injury to cause upregulation and translocation of transcription factor NFATc3 to the nuclei of endothelial, smooth muscle and adventitial cells was assessed in exposed ventral arteries crushed in situ for 5 s with a surgical hemoclamp. Crushed arteries from 8 rats were fixed for immunostaining either 5 or 45 min following injury.

RESULTS

Vibration Model. Rats accommodated to the restraint tubes with minimal struggling and displayed only a brief startle response of the head when the vibration platform was activated. Plastic splints held the tails against the vibration plate with slight, but nondamaging, compression (Fig. 1A,B). Lack of splint-induced damage was indicated by the absence of skin abrasions and persistent "healthy pink" coloration of the tails throughout 9 days of treatment for all of the sham control and vibrated rats.

Transcription Factor Immunolocalization. NFATc3 immunostaining of nonvibrated, normal arteries was negative and indistinguishable from the omission of

primary antibody control for all rats (Fig. 2A). Arteries fixed 45 min after performing the positive control of a mechanical crush exhibited NFATc3 immunofluorescence in the cytoplasm and nuclei of endothelial, smooth muscle, and adventitial connective tissue cells (Fig. 2B). No signal was detected in arteries fixed 5 min after crushing, indicating that upregulation of NFATc3 required protein synthesis (data not shown). A single bout of 4-h vibration produced dramatic increases in NFATc3 immunostaining in the cytoplasm and nuclei of endothelial cells in all of eight rats (Fig. 3A). Counterstaining DNA in the immunoreacted sections with propidium iodide confirmed nuclear localization of NFATc3 in a subset of cells (Fig. 3B). NFATc3 immunostaining was not present in any of the eight arteries removed 45 min after cessation of vibration on the 9th day (Fig. 3C). Sham controls (1-day and 9-day) displayed NFATc3 levels equivalent to background, demonstrating that handling and experimental procedures without vibration did not trigger expression of this marker.

Electron microscopy showed that all eight sham control arteries examined possessed a continuous endothelium (Fig. 4A). One day of vibration resulted in double membrane limited vacuoles within a subset of cells in a continuous endothelium in all eight vibrated arteries (Fig. 4B,C). Following 9 days of vibration, regions of missing endothelial cells were common in every vibrated rat (Fig. 4D). Endothelial cells bordering denuded regions extended thin processes and partially covered the exposed extracellular matrix (Fig. 4D). The internal elastic membrane was frequently missing or attenuated at injury sites (Fig. 4E). Endothelial cells bordering the exposed connective tissue regions were typically necrotic and fragmented with adhering activated platelets. Swollen vacuoles with double limited membranes also occurred in the smooth muscle cells of all vibrated arteries following 1-day and 9-day treatment (not shown). These large vacuoles were rarely observed in endothelial and smooth muscle cells of controls.

Tail Tissue Blood Perfusion. Laser doppler blood flow monitoring revealed that 5 min of vibration caused a significant ($P < 0.01$, paired t-test) decrease in tissue perfusion units for all five vibrated animals. The mean decrease was 37 ± 1% for pre- to post-vibration perfusion levels.

DISCUSSION

Early Consequences of Vibration. The present study demonstrates that endothelial cells show signs of injury after a single 4-h bout of vibration. This progressed to extensive endothelial cell death after 9 days of vibration. These results indicate that vascular injury is an early event in the process of vibration injury.

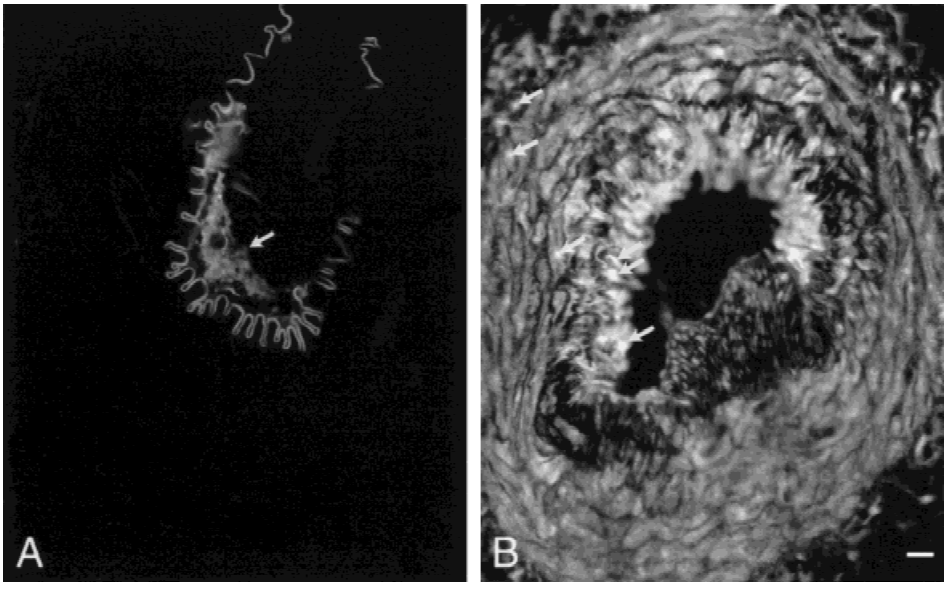

FIGURE 2. Cross-sections of normal **(A)** and crush-injured **(B)** tail arteries were reacted by indirect immunofluorescence for NFATc3 transcription factor protein. The injured artery was fixed 45 min following compression. The normal control artery lacks specific labeling. The folded internal elastic membrane is autofluorescent, and blood (arrow in **A)** in the lumen exhibits nonspecific fluorescence. Panel **(B)** illustrates that injury induced cytoplasmic and nuclear (arrows) immunolabeling of cells in the intima, media, and adventitia. This staining was absent when the primary antibody was omitted (not shown). Bar = 150 μm for both sections.

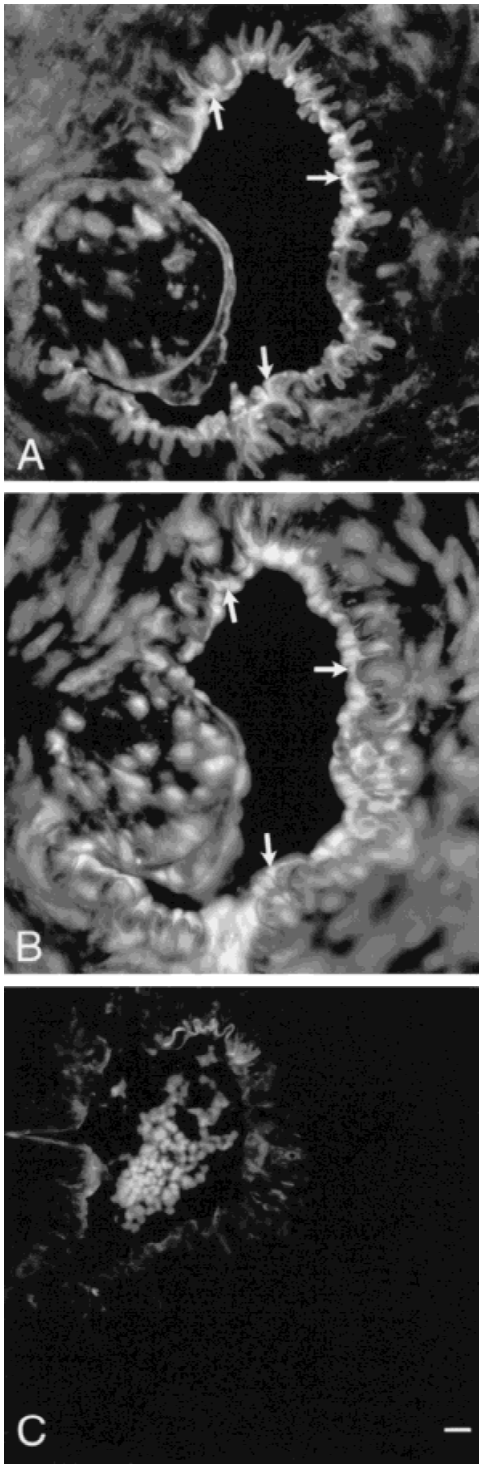

FIGURE 3. (A) After 4 h of 60 Hz, 49 m/s^2 vibration, fluorescein immunofluorescence staining of NFATc3 occupies the cytoplasm and nuclei (arrows) of many endothelial cells in the ventral tail artery. **(B)** Fluorescence imaging of the same section for propidium iodide-stained DNA confirms nuclear localization (arrows) of NFATc3. **(C)** NFATc3 is not detectable in arteries vibrated for 9 days. Blood in the lumen stains nonspecifically. Bar = 150 μm for all panels.

Upregulation of NFAT. When the present investigation was initiated, there were no reports of suitable early markers for vibration-induced cell injury. From our screening of a large number of antibodies recognizing immediate early-type proteins (cfos, cjun, cjun-P, NFATc1– NFATc3), NFATc3 proved a sensitive and appropriate marker for cell injury for the following reasons: (1) baseline immunostaining levels in normal arteries were extremely low, (2) a robust response occurred within 45 min of cell injury, and (3) most importantly, all cell types in the initima, media, and adventitia were capable of displaying a positive response when injured.

In this study, NFATc3 was used simply as a marker for early cell damage. NFAT was detected in the nuclei of many, but not all, responding cells. Time residence in the nucleus is brief and may explain why nuclear localization was not seen in some cells.[30] In the nucleus, NFATc3 appears to have promoted auto-upregulation because elevated immunostaining was never detected 5 min after crush, whereas after 45 min strong staining was present. The delayed appearance is consistent with time required for transcription and translation of new protein and rules out rapid unmasking of a pool of preexisting transcription factor.

NFAT has been shown to regulate cardiac hypertrophy, to play a role in long-term memory in neurons, and to be involved in the control of interleukin-3 production.[4,7,15] In the vibration-injured tail arteries, endothelial cells are likely to show a unique set of NFAT stimulated genes. Characterizing the mechanism of action and the protein expression induced by NFAT is beyond the scope of the present study. This approach would be important for future studies that continue probing the cellular and molecular mechanisms of vibration injury.

Postulated Mechanism of Injury. It was unexpected that NFATc3 was not upregulated in endothelial cells after 9 days of vibration because EM revealed cell damage greater than that seen after 1 day. One interpretation is that the type of endothelial damage that upregulates NFATc3 only occurs in the earliest stages of vibration injury. Days later, cell death may result from acute necrosis and apoptosis not associated with immediate early gene or NFAT expression.

Inspection of the distribution of endothelial cells expressing NFATc3 at 1 day suggests that a subset of endothelial cells are susceptible to injury. This heterogeneity, if substantiated by further study, is interesting because experiments in which norepinephrine was directly applied onto the saphenous and medial tarsal arteries in rats showed two populations

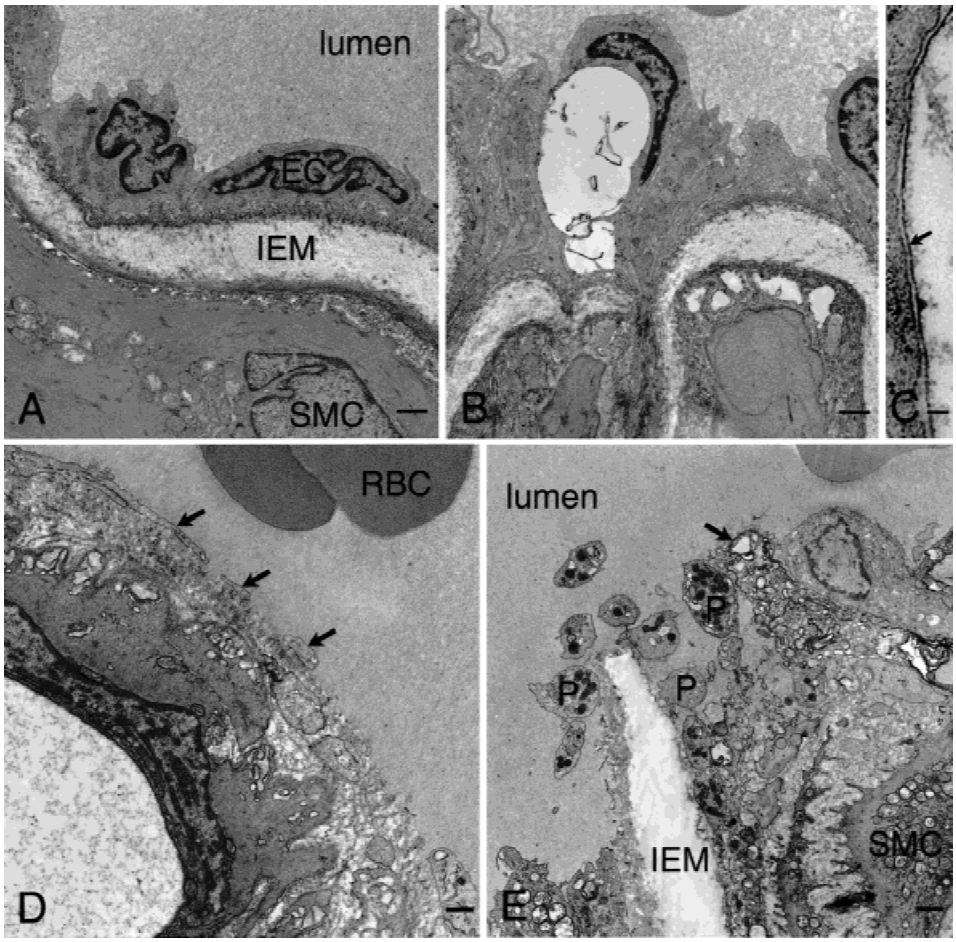

FIGURE 4. (A) In the electron micrograph of a nonvibrated artery, a continuous layer of endothelial cells (EC) separates blood in the lumen from the underlying internal elastic membrane (IEM) and smooth muscle cell (SMC). **(B)** Following 1 day of vibration, endothelial cells in the vibrated artery contain large vacuoles not present in controls. **(C)** The vacuoles are limited by double membranes (arrow). **(D)** After 9 days of vibration, the endothelium is discontinuous, and thin processes (arrows) of endothelial cells partially cover the exposed connective tissue (RBC, red blood cells). **(E)** The lesion site shows denuded endothelium, adherence of activated platelets (P) to the exposed connective tissue, a disrupted IEM, and a degenerating endothelial cell (arrow). Bar = 1 μm for **(A)**, 1 μm for **(B)**, 0.05 μm for **(C)**, 0.5 μm for **(D)**, and 0.75 μm for **(E)**.

of endothelial cells: those distributed on the hills and those in the valleys of the internal elastic membrane.[10] Cells residing in the valleys appeared mechanically-pinched in the hyperconstricting arteries when the internal elastic membrane was folded very tightly. In our study, cells on the crests of hills appear to express NFATc3, whereas the valley cells do not. The valley cells may never recover from the repetitive mechanical trauma, undergo cell death, and produce the denuded spots observed at 9 days. The altered state of the endothelium at 9 days may spare the remaining cells from the stresses that signaled NFATc3 expression earlier. To address this issue, temporal changes in the endothelium will be examined. For a mechanical pinching mechanism to operate, the rat tail artery must vasoconstrict in response to vibration.

Vasoconstriction Model of Vibration Injury. Following 1 day of vibration, large vacuoles enclosed by two membranes are present in the endothelial and smooth muscle cells of vibrated arteries. These vacuoles are morphologically similar to those formed under the extreme vasoconstriction generated by direct norepinephrine application.[11] The similarity of vacuole morphology suggests that vibration induces vasoconstriction of the tail artery. Further support for vasoconstriction is provided by surface laser doppler showing a 37% reduction in tissue blood perfusion following 5 min of vibration. Interestingly, vibrated human fingers exhibit similar early decrements in blood perfusion.[33] Implanting doppler flow probes on the tail artery is needed for direct demonstration of reduced blood flow and the longer-term hemodynamic changes.

Effects of Vibration on Vascular Smooth Muscle. Previous vibration studies reported no change in vascular smooth muscle until 60 days.[19] However, after 9 days of vibration, we observed subtle indications that smooth muscle cells respond by expressing an enhanced secretory phenotype. Chondroitin sulfate proteoglycan, which increases prior to smooth muscle migration,[22] appears elevated in the extracellular matrix between smooth muscle cells (Curry 2000, unpublished observations).

Denuding endothelial cells during balloon angioplasty has revealed that breakdown of the endothelial barrier triggers platelet adherence and secretion of factors that degrade the internal elastic membrane.[24] Growth factors from platelets and blood lead to smooth muscle proliferation and restenosis.[2,25] A similar scenario may transpire when vibration disrupts the tail artery endothelium and causes degradation of the internal elastic membrane. If correct, vibrating beyond 9 days should lead to smooth muscle overgrowth and vascular occlusion. This would account for the deficient peripheral circulation in secondary Raynaud's disease.

Neural Involvement in Vibration Injury. Vibration-injured workers with endstage HAVS disease exhibit peripheral nerve degeneration as well as vascular deficits. There is myelin damage, loss of nerve fibers, Schwann cell proliferation, and perineurial fibrosis.[26,27] Rabbits standing on a vibration platform accelerating at 60 Hz and 51 m/s^2 for 2 h/day, 6 days/week for 600 h show severe vacuolization in the median nerve.[9] Sciatic nerves of anesthetized rats exposed to 82 Hz vibration and an acceleration of ~28 m/s^2 for 4 h/day for 5 days exhibit epineurial edema.[13] These data indicate that neurological damage can begin as early as 5 days. Endothelial cell vibration injury occurs after 1 day in the tail artery. Tail nerves from the same groups of rats are being examined ultrastructurally to ascertain whether nerve degeneration occurs simultaneously with vibration-induced vascular injury.

Utility of the Rat Tail Vibration Model. A rat tail model of vibration injury was exploited to identify the earliest cell types affected by 60 Hz, 5 g acceleration. Other frequencies, accelerations, and durations can be tested to determine which parameters of vibration disrupt tissue integrity. Powered tool vibration is very complex and multifaceted, making it extremely difficult to link acceleration parameters to specific types of injuries. In the workplace, overgripping and decreased temperature exacerbate HAVS.[23] Rat tail vibration may be used to simulate this complex situation by cooling the tail and activating tail muscle contractions with nerve stimulation during vibration. Our initial strategy sought to identify the earliest cells impacted negatively by vibration in a simplified defined environment. The findings support the belief that endothelial damage results from vibration-induced vasoconstriction.

The authors thank James R. Jaeschke for help with vibration. This work was supported by NIOSH grant R01 OH03493.

REFERENCES

1. Abbruzzese M, Loeb C, Ratto S, Sacco G. A comparative electrophysiological and histological study of sensory conduction velocity and Meissner corpuscles of the median nerve in pneumatic tool workers. Eur Neurol 1977;16:106–114.
2. Brady AJ, Warren JB. Angioplasty and restenosis. BMJ 1991; 64:351–353.
3. Cohen SR, Bilinski DL, McNutt NS. Vibration syndrome. Arch Dermatol 1995;12:1544–1547.
4. Duncliffe KN, Bert AG, Vadas MA, Cockerill PN. A T cell-specific enhancer in the interleukin-3 locus is activated cooperatively by Oct and NFAT elements within a DNase I-hypersensitive site. Immunity 1997;6:175–185.
5. Farkkila M, Pyykko I, Jantti V, Aatola S, Starck J, Korhonen O. Forestry workers exposed to vibration: a neurological study. Br J Ind Med 1988;45:188–192.
6. Futatsuka S, Ueno T, Sakurai T. Follow up study of vibration induced white finger in chain saw operators. Br J Ind Med 1985;42:267–271.
7. Graef IA, Mermelstein PG, Stankunas K, Neilson JR, Deisseroth K, Tsien RW, Crabtree GR. L-type calcium channels and GSK-3 regulate the activity of NF-ATc4 in hippocampal neurons. Nature 1999;401:703–708.
8. Hamilton A. A study of spastic anemia in the hands of stonecutters: the effects of the air hammer on hands of stonecutters. Washington DC: U.S. Dept of Labor; 1918. Report 236, No. 19.
9. Ho ST, Yu HS. Ultrastructural changes of the peripheral nerve induced by vibration: an experimental study. Br J Ind Med 1989;46:157–164.
10. Joris I, Majno G. Endothelial changes induced by arterial spasm. Am J Pathol 1981;102:346–358.
11. Joris I, Majno G. Medial changes in arterial spasm induced by L-norepinephrine. Am J Pathol 1981;105:212–222.
12. Juntunen J, Taskinen, H. Pathogenic and clinical aspects of polyneuropathies, with reference to hand-arm vibration syndrome. Scand J Work Environ Health 1987;13:363–366.
13. Lundborg G, Dahlin LB, Danielsen N, Hansson HA, Necking LE, Pyykko I. Interneural edema following exposure to vibration. Scand J Work Environ Health 1987;13:326–329.
14. Matloub HS, Kolachalam RB, Garancis JC, Yousif NJ, Sanger JR, Van Over JE. Vibration syndrome: is there neurological injury? Abstract, 44th annual meeting of the American Society for Surgery of the Hand, Seattle, Washington, 1989.
15. Musaro A, McCullagh KJ, Naya FJ, Olson EN, Rosenthal N. IGF-1 induces skeletal myocyte hypertrophy through calcineurin in association with GATA-2 and NF-ATc1. Nature 1999; 400:581–585.
16. Necking LE, Lundstrom R, Lundborg G, Thornell LE, Friden J. Skeletal muscle changes after short term vibration. Scand J Plast Reconstr Surg Hand Surg 1996;30:99–103.
17. Ogasawara C, Sakakibara H, Kondo T, Miyao M, Yamada S, Toyoshima H. Longitudinal study on factors related to the course of vibration-induced white finger. Int Arch Occup Environ Health 1997;69:180–184.
18. Okada A. Physiological response of the rat to different vibra-

tion frequencies. Scand J Work Environ Health 1986;12: 362–364.
19. Okada A, Inaba R, Furuno T. Occurrence of intimal thickening of the peripheral arteries in response to local vibration. Br J Ind Med 1987;44:470–475.
20. Olsen N, Nielsen SL. Vasoconstrictor response to cold in forestry workers: a prospective study. Br J Ind Med 1988;45: 39–42.
21. Pyykko I, Gemme G. Pathophysiological aspects of peripheral circulatory disorders in the vibration syndrome. Scand J Work Environ Health 1987;13:313–316.
22. Rabinovitch M. Cell–extracellular matrix interactions in the ductus arteriosis and perinatal pulmonary circulation. Semin Perinatol 1996;20:531–541.
23. Radwin RG, Armstrong TJ, Chaffin DB. Power hand tool vibration effects on grip exertions. Ergonomics 1987;30: 833–855.
24. Ross R, Glomset J, Harker L. Response to injury and atherogenesis. Am J Pathol 1977;86:675–684.
25. Shirotani M, Yui S, Kawai C. Restenosis after coronary angioplasty: pathogenesis of neointimal thickening initiated by endothelial loss. Endothelium 1993;1:5–22.
26. Tacheuchi T, Futatsuka M, Imanishi H, Yamada S. Pathological changes observed in the finger biopsy of patients with vibration-induced white finger. Scand J Work Environ Health 1986;12:280–283.
27. Takeuchi T, Futatsuka M, Imanishi H, Yamada S. Ultrastructural changes in peripheral nerves of the fingers of three vibration-exposed persons with Raynaud's phenomenon. Scand J Work Environ Health 1988;14:31–35.
28. Taylor JS. Vibration syndrome: a missed diagnosis. Occup Med 1986;1:259–272.
29. Thompson J. Parallel spindle systems in the small muscles of the rat tail. J Physiol 1970;211:781–799.
30. Timmerman LA, Clipstone NA, Ho SN, Northrop JP, Crabtree GR. Rapid shuttling of NF-AT in discrimination of Ca^{2+} signals and immunosuppression. Nature 1996;383:837–840.
31. Tseng HM, Yu HS, Ho ST, Yao TH. Vibration syndrome—pathophysiological and electronmicroscopic studies. Kashsiung J Med Sci 1986;2:732–744.
32. Wasserman D, Badger D, Doyle L. Industrial vibration—an overview. J Am Soc Safety Eng 1974;19:38–43.
33. Welsh CL. The effects of vibration on digital blood flow. Br J Surg 1980;67:708–710.
34. Wu Y, Jiji LM, Lemons DE, Weinbaum S. A non-uniform three dimensional perfusion model of rat tail heat transfer. Phys Med Biol 1995;40:789–806.